Helmholtz-Zentrum Geesthacht
Zentrum für Material- und Küstenforschung

Final Draft
of the original manuscript:

Paul, J.D.H.; Lorenz, U.; Oehring, M.; Appel, F.:
Up-scaling the size of TiAl components made via ingot metallurgy
In: Intermetallics (2012) Elsevier

DOI: 10.1016/j.intermet.2012.08.006

Up-scaling the Size of TiAl Components made via Ingot Metallurgy

J.D.H. Paul, U. Lorenz, M. Oehring, and F. Appel
Institute of Materials Research, Helmholtz-Zentrum Geesthacht, D-21502 Geesthacht, Germany.

Corresponding author: Jonathan D.H. Paul, e-mail: jonathan.paul@hzg.de
Phone: +49 4152 872511, FAX: +49 4152 872534
e-mail addresses: uwe.lorenz@hzg.de
michael.oehring@hzg.de
fritz.appel@hzg.de

Abstract

The quality of wrought discs made from large Ti-45Al-5Nb-0.2B-0.2C (at. %) ingots has been assessed at various stages of processing. Such components suffer from different types of defects that can usually be traced back to structural and chemical inhomogeneities that are present in the starting ingot. In conventional manufacturing routes the imparted mechanical strain is often insufficient for complete dynamic recrystallisation, particularly for large parts. In an attempt to overcome these problems, a new multi-stage method has been developed, which has the advantages that:

i) the strain is significantly higher than that imparted using conventional routes,

ii) the flow direction of the material is inverted between the first and second processing stages in the sense that the length of the ingot is first increased via extrusion, and then the resulting extruded bar is shortened via axial forging in the subsequent processing stages, and

iii) the geometrical constraints associated with the production of large components from ingots can be overcome.

The reliability of the method has been assessed by metallographic and mechanical characterisation. The challenges that have to be addressed for the new technique to be employed for the manufacture of large components are discussed.

Keywords: A. titanium aluminides, based on TiAl. C. isothermal forging. C. joining. D. microstructure. F. mechanical testing.

1 Introduction

It is well established that the properties of γ-TiAl alloys are highly dependent on composition and microstructure. An inhomogeneous microstructure resulting from chemical inhomogeneity within a component can lead to a large scatter in mechanical properties. This is undesirable and can result in components being over-designed so that minimum properties can be guaranteed. For parts produced through ingot metallurgy, any chemical segregation during ingot solidification is very difficult to remove, requiring heat-treatment at temperatures within the alpha phase field or even higher. Defects such as cracks, inclusions based on titanium, niobium or other refractory elements, or even porosity may be present within ingots. The extent of such defects and elemental macro-segregation is magnified as ingot size increases. These inherent problems make the production of large parts, with guaranteed properties and homogeneous microstructures, much more challenging. Hot working technologies, such as extrusion or forging, either singularly or combined, are often used to improve the mechanical properties of ingot-based material. The first part of the paper assesses quality issues associated with the application of such conventional techniques during the production of wrought Ti-45Al-5Nb-0.2B-0.2C material from large ingots. Processing of this type of alloy composition is particularly demanding because of its good high temperature strength retention [1] that arises because of the low aluminium content and the high content of the slowly diffusing element niobium [2]. A general difficulty associated with hot-working is the limited ability to impart large amounts of strain while maintaining sizes that are similar to component dimensions. Thus the production of large high quality components, such as discs, from ingot material presents significant difficulties. The second part of the paper demonstrates and discusses a new method, that is easy to upscale, in which defect-containing ingots can be processed to potentially "defect-free" components. A large disc that was manufactured using the newly developed technique was thoroughly characterised in terms of microstructure, chemical homogeneity, defect types and tensile properties. Finally, the challenges for an affordable application of the new technique to produce large wrought products are discussed.

2 Experimental procedure

2.1 Primary processing

Two large vacuum arc melted ingots with approximate dimensions of 220 mm diameter ($A_o \approx 380$ cm^2) and 750 mm length with the nominal composition Ti-45Al-5Nb-0.2B-0.2C were used in the study. These were encapsulated in steel cans with a molybdenum interlayer to prevent any reaction between the outer canning material and the TiAl. The billets were pre-heated at 1250°C and then extruded (Special Metals, Hereford, UK) to round bars with diameters of 90 mm; the TiAl extrudate having a diameter of roughly 77 mm ($A_f \approx 47$ cm^2). Thus the extrusion ratio ($R=A_o/A_f$) for the TiAl

was around 8.2:1 and the corresponding reduction ratio ($r = ((A_o - A_f)/A_o) \times 100$) around 88%. The extruded bars were annealed for 2 hours at 1030°C followed by furnace cooling. A specimen was cut from one of the extruded bars and a metallographic section of a face parallel to the extrusion direction, passing through the middle of the bar, was prepared for scanning electron microscopy. Small forging billets with dimensions of 70 mm diameter by 110 mm height were machined from the remaining annealed extruded bars. These were subsequently isothermally forged (Leistritz Turbinenkomponenten, Remscheid, Germany) using a strain rate of 5×10^{-3} s^{-1} at a nominal temperature of 1150°C to discs with approximate dimensions of 170 mm diameter and up to 20 mm in thickness (a reduction of around 82%). Prior to further processing the forged discs were annealed at 1030°C for 4 hours.

2.2 HIP bonding and subsequent isothermal forging

Cylindrical plates with diameters of 14.5, 15.0 or 15.5 cm were cut from the annealed forged discs and their end faces ground so that they were parallel with disc thicknesses ranging from 14 to 19 mm. These were thoroughly cleaned before being stacked one on top of another and then joined by HIP diffusion bonding. This was done by encapsulating the stacked discs in a can, made from 1 mm thick titanium sheet, which was then evacuated and sealed. HIP bonding was performed at a temperature of 1200°C for 4 hours under argon gas at a pressure of 200 MPa. The HIPed assemblies were then used as forging billets that had heights of 80 mm, 135 mm and 150 mm, respectively. These were isothermally forged at 1150°C using a strain rate of 5×10^{-2} s^{-1} to final thicknesses of around 38 mm (Ladish Forge, Milwaukee, USA). In total three large discs were successfully manufactured using this technique.

2.3 Metallographic characterisation and mechanical testing

The wrought products at different stages of manufacturing were sectioned for metallography and both metallographic and tensile test specimens were made from the second largest forged disc. All scanning electron microscopy was performed in a Zeiss Gemini microscope equipped with a system (EDX) for chemical analysis. The EDX system was calibrated with an alloy standard that had been prepared from an argon-arc melted button. EDX measurements on a series of similarly prepared alloys showed that the aluminium concentration could be determined to ± 0.1 at. %. In this work, only the Ti, Al and Nb concentrations were determined by EDX and normalised to 100 at. %, since the B and C contents cannot be reliably measured. Room temperature tensile tests were performed on an MTS universal testing machine at a strain rate of 2.38×10^{-5} s^{-1} in strain controlled mode or at an initial strain rate of 2.38×10^{-5} s^{-1} in displacement controlled mode.

3 Results and Discussion

3.1 Microstructure after ingot conversion

3.1.1 Extrusion

Micrographs that indicate the variation of microstructure across the extruded bar after annealing are shown in Figs. 1 and 2. As can be seen in Fig. 1a the microstructure in regions away from the centre of the bar consisted of a mixture of coarse and fine grained bands. Figure 1b shows a boundary region between an area of fine and coarse grained microstructure in higher magnification. The composition of the whole area shown in Fig. 1b, as well as the composition of the fine-grained upper region and coarse-grained lower region of the microstructure, was determined using EDX analysis. The composition of the fine microstructure within the upper half of the micrograph (Fig. 1b) was Ti-46.9Al-4.9Nb while that determined for the coarser microstructure in the lower half of the micrograph was Ti-47.6Al-4.7Nb. For Al, these values lie on either side that determined for the whole area, Ti-47.2Al-4.7Nb. On careful examination of Fig. 1b it can be seen that many more boride particles (or remains of borides after electro-polishing) were present in the coarser Al-rich microstructure. This observation indicates that boron-enriched melt or boride precipitates segregate to the Al-enriched interdendritic regions during ingot solidification as expected from the ternary Al-B-Ti phase diagram [3], and that the interdendritic regions are quite large. On moving towards the centre of the annealed extruded bar, the microstructure changed to a predominantly lamellar microstructure, Fig. 2, although fine-grained microstructural regions were present between the lamellar areas.

In an attempt to explain the microstructural variation between the outer and central regions of the bar, a composition profile was made across the extruded bar, passing through its centre. This was done by performing a series of individual EDX analyses on 1.08 mm^2 areas at 2 mm intervals across the specimen taken from the annealed bar. The resulting Al and Nb profiles across the bar are shown in Fig. 3. As can be seen the aluminium varies from levels of around 48 at.% near the outer surface of the bar to levels of 45 at.% near the centre of the bar. The variation of Nb is more complicated than that of aluminium. Near the outer surface the niobium content is relatively low at around 4.4 at.% Nb; this is 0.6 at.% below the nominal value for the alloy. On moving towards the centre, the niobium contents increases rapidly to around 5.3 at.% before reducing to its nominal value of 5 at.% in the central region of the bar. Due to the fact that during extrusion the central portion of the ingot is pushed forward compared to the outer regions, the compositional variation determined across the extruded bar is determined by both the centre to surface, and to some extent,

the end to end composition variations within the cast ingot. The measured variation of Al, which arises due to solidification, can explain the microstructural variations across the bar. Similarly the variation of Nb across the bar also reflects the segregation resulting from the VAR ingot manufacture. To be able to make a more detailed description of the reasons behind the elemental segregation within the piece of extruded bar examined (and also for any other positions along the bar) would require an extensive examination of the segregation within the starting ingot or within a similarly manufactured ingot of the same composition and size. Obviously the first option is not possible because it would not then be possible to extrude the sectioned ingot. The second option is prohibitively expensive, an ingot costing anything upwards of $15000, and there is no guarantee that the segregation, which as discussed later depends on the size and distribution of the starting components, will be exactly reproducible. Obviously any large differences in composition and microstructure are undesirable.

3.1.2 Extrusion plus single-step forging

After the 110 mm long billets of extruded material had been isothermally forged, the microstructure was fully recrystallised with no remaining lamellar colonies being observed in the forging that was examined. Figure 4 shows that the microstructure within such a forged disc contains banded areas of fine ($\alpha_2 + \gamma$) duplex microstructure together with slightly coarser areas of mainly γ phase. The orientation of the bands seemed to depend on their position within the disc. Towards the outer rim these bands were generally orientated perpendicular to the forging direction, Fig 4a, whereas towards the centre of the disc, near to the forging-die/billet contact faces, their orientation seemed parallel to the forging direction, Fig 4b. On moving away from this central face region towards the centre of the disc, the orientation of the microstructural bands gradually changed from being parallel to being perpendicular to the forging direction. This observation probably results from a "dead zone" close to the forging dies restricting deformation to levels lower than that required to re-orientate the pre-existing as-extruded microstructure of the forging billet. Data concerning the distribution of aluminium and niobium across an annealed forged disc, from rim to rim, is shown in Fig. 5. The distribution of Al across the disc is much more uniform than observed across the extruded bar, but areas that differ in Al by up to 2 at.% are still present. Also the mean aluminium level is around 1 at.% higher than the nominal value. Given the marked elemental segregation determined across the bar (Fig. 3), it is difficult to explain the more uniform segregation across the small forged disc. The isothermal forging processing and the associated high temperatures are unable to provide the necessary diffusion necessary to even-out such macro-segregation. It can only be speculated that the compositional variation across the extruded bar varies along its length. This

would depend on the extent and the pattern of segregation within the starting ingot which are unknown.

3.2 Three-stage hot-working

3.2.1 Imparted strain

The large forged discs that were produced by isothermally forging the bonded stacks (of smaller discs) are shown in Fig. 6a, while Fig. 6b shows an assembly of small forged discs that were used to make the stacked assemblies prior to HIP bonding. The manufacture of such large TiAl components presents significant difficulties as explained earlier. One important factor, relevant to the degree of microstructural conversion of an ingot via hot working, is the amount of imparted deformation. With conventional technologies it is difficult to impose sufficiently large amounts of deformation to refine the coarse as-cast ingot microstructure of large ingots, while simultaneously retaining dimensions that are big enough to manufacture large components. This is particularly problematic for large disc-shaped geometries. The degree of hot work imposed on the material in the present investigation can be estimated by calculating the true strain, ε_t:

$$\varepsilon_t = \ln(h_1/h_2)$$

where h_1 and h_2 are the lengths of the work-piece before and after hot working. The sum of the true strain deformations that were imparted during the individual deformation processes during manufacture of the 3 large discs, i.e. during extrusion, initial isothermal forging and subsequent isothermal forging, ranges from 4.54 to 5.17. Similar levels of deformation within such large, crack-free, pieces of titanium aluminide have never been previously reported; indicating the innovation of the technique developed, for which patents have been granted [4]. The high level of imparted deformation is the main reason for the very fine as-forged microstructure which, as described later, was present throughout the large disc that was examined.

High levels of deformation have been achieved in more conventional lightweight materials, such as aluminium and magnesium, via equal channel angular extrusion (ECAE). This method has the advantage that the specimen dimensions remain more or less unchanged after processing. The technique has also been applied to process TiAl in a number of studies [5-7]. However the maximum specimen volume used in these studies was no greater than 52 cm^3, i.e. very much smaller than ingots required to make large components. Although sub-micron microstructures could be developed; even using such small specimen sizes the technique was found to be very challenging due to flow localisation, shear band development and cracking [5]. An alternative technique that

showed great promise using small scale specimens, involved combined torsional and compressive deformation [8]. While the technique was successfully applied for the further consolidation of extruded material, it was difficult to use for ingot material because highly localised shear bands developed and acted as crack initiation sites [9]. Using double extrusion, Draper et al. [10] achieved high levels of deformation in crack-free material of the same composition as used in the current investigation. The total extrusion ratio was 100:1 which is equivalent to a true strain of around 4.6. This level of deformation is very similar to that imparted into the 3 large discs manufactured in this investigation, but it was achieved at the expense of the diameter of the bar which thereafter was only suitable for making long thin components. Thus the technique outlined in this publication is the only one able to demonstrate full breakdown of the as-cast microstructure and formation of a fine grained microstructure throughout a large disc-shaped part. The paper will now concentrate on characterising the microstructural inhomogeneities and defects within the large disc, as such features give rise to reduced property reliability.

3.2.2 Microstructure after three-stage hot working

It was decided to investigate the microstructure and mechanical property of the second largest disc. The smallest disc was deemed as being a little too small for obtaining suitable tensile test-piece specimens, while the largest disc has been saved for later manufacture of a turbine disc or BLISK. Microstructures observed within the second largest as-forged disc are shown in Fig. 7. Similar to the small forged discs, the microstructure consists of duplex areas containing both lighter and darker phases ($\alpha_2+\gamma$) and areas made up of mainly darker γ phase. Once again some areas showed a particular alignment of the microstructure with respect to the forging direction (Fig. 7a) while other areas exhibited a less obviously orientated “mottled” microstructure (Fig. 7b). The mottling consists of areas of mixed ($\alpha_2+\gamma$) and other areas of mainly darker γ phase. The local orientation may depend on both shear processes during secondary forging and the initial orientation of the microstructure in the small forged discs, and is thus likely to depend on position.

The second largest disc shown in Fig. 6a demonstrated a technical complication that can frequently occur during forging and could be a quality issue. The problem is manifested close to the disc rim with the aligned microstructural regions close to the upper face of the disc not being orientated perpendicular to the forging direction, but curved upwards so that they intersected the outer rim surface at an angle of around 90°. This is probably due to the upper die of the isothermal forge being marginally colder than the lower die; or possibly the die lubrication not being as efficient as for the lower die. This was seemingly not the case for the other two large forged discs which exhibited symmetrical rim profiles. For the largest disc the rim profile was roughly parallel to the forging direction along its entire length, indicating that the lubrication technique employed to

reduce friction between the die and the workpiece was very effective and that the die temperatures were the same.

In some cases the joining interfaces were recognisable in the large disc because compositional differences of adjacent stacking elements gave rise to microstructural differences. Such an interface, which is formed by HIP-bonding small discs of somewhat different compositions, is shown in Fig. 8a together with the results from an EDX analysis line scan across the interface, Figs. 8b and 8c. From Fig. 8b it can be seen that the aluminium concentration gradually reduces along the line scan. By determining the mean aluminium concentration on each side of the boundary, the position of which can be deduced from the abrupt step in niobium concentration values, it was found that the mean aluminium concentration on each side of the boundary differed by around 1 at.%. Similarly the mean niobium concentration varied by 0.5 at. %, with the higher mean niobium level being measured in the material with the lower mean aluminium concentration. It should be mentioned that no quality limiting features such as pores, oxides or α_2 layer were observed at the interface as has been reported at diffusion bonded joints [11].

In addition to the above described microstructural feature that arose in the large disc at the boundaries between two adjacent stacking elements; other very significant microstructural variations that probably originated within individual stacking elements were found. These features will now be described. Figure 9 shows an extreme area of segregation and the associated elemental line scans. Although a very significant compositional variation is associated with this segregation, it should be mentioned that the region of aluminium enrichment was rather limited and did not extend over a large length. This probably indicates that it was located within just one of the original stacking discs, rather than at a joint between adjacent stacking elements. It is likely that such a region of enhanced aluminium originated from a large volume of interdendritic material that formed during ingot manufacture.

Another feature, consisting of a large band defect that was present within an otherwise fine near alpha-transus heat-treated microstructure, is shown in Fig. 10. Although this defect was less than 100 μm in width, it was several mm in length, and even visible to the naked eye. Figures 10b and 10c show where EDX (point) line scans were performed both transverse to and along the band defect. The results of these scans are shown in Figs. 10d and 10e respectively. The elemental line scan across the band (Fig. 10d) indicates that the fine microstructure on either side of the band is composed of the α_2 and γ phases. The apparent scatter in Al concentration results from the analysis spot of the electron beam interacting with a certain volume of material that is composed of mostly

(or completely) γ phase (high measured Al concentration) or a mixture of both the α_2 and γ phases. Naturally the degree of scatter depends on both the size of the spot and the respective phases. The scan clearly indicates the position of the band, and shows a very small scatter in Al concentration within the band which is probably a consequence of the extremely fine scale of its microstructure. Using all the analyses points determined for the scan that lie within the band, its mean composition was determined to be Ti-43.6Al-5.5Nb. The scan along the band (Fig. 10e) indicated a mean composition of Ti-42.6Al-5.1Nb. Interestingly there seems to be a relationship between the local variation of niobium and aluminium. As can be seen in Fig. 10e, a local increase or decrease of the niobium concentration is mirrored by an increase or decrease of the aluminium concentration. This trend is unlike what would be expected from solidification where aluminium is usually enriched in the inderdendritic regions and niobium at dendrite cores.

Thus the origin of this band defect is not immediately obvious, but a similar type of defect in the as-forged material, but probably at an earlier stage of development is shown in Fig. 11. As can be seen, this defect is composed of a number of rounded inclusions, three of which are apparently connected by a thin layer of material. The composition determined for a relatively large area of the largest inclusion on the left hand side of the micrograph was Ti-30.7Al-4.4Nb while the neighbouring matrix had the composition Ti-46.1Al-5.1Nb. The development of such defects via segregation during solidification seems very unlikely; rather it would seem that they are partially reacted remnants of material that was used to make the initial VAR electrode, as discussed in the next section.

Figure 12a shows another defect found in the large disc that was visible to the naked eye, appearing as a small crack on the metallographic surface. As can be seen in Fig. 12b, the defect is actually an inclusion, separated from the matrix by a thin reaction zone. EDX mapping analysis showed this inclusion to be rich in titanium and carbon, thus indicating it to be a TiC based inclusion. The reason for the formation of such an inclusion is not immediately obvious; a possible explanation for its presence will be given in the next section.

3.3 Origin of inclusion-like defects

During the metallographic investigation of the large forged disc and mechanical testing, three types of inclusion-like defects were found. Such defects could compromise the mechanical properties. The defects can be classified as localised areas with a very low aluminium concentration (Figs. 10 and 11), a large TiC based particle (Fig. 12), and a multi-phase defect (Fig. 13). The reason for the presence of low aluminium containing inclusions is probably due to insufficient mixing during the

ingot melting process. On account of their higher titanium content, the melting point of such defects is probably somewhat higher than that of the surrounding matrix. If such material is surrounded by aluminium rich material within the VAR electrode, then it could easily fall into the melt, remaining relatively intact and un-mixed. Of course, if such material remained within the melt for a long time, then it may begin to dissolve; however this would depend on the exact ingot processing conditions. Similarly to the study by Godfrey and Loretto [12] for PAM ingot processing, it is very likely that the size of the elemental and master-alloy starting materials used to make the initial VAR electrode plays a significant role. Similarly the multi-phase defect found on the fracture surface of one of the broken tensile test specimens (Fig. 13) probably originates from a master-alloy component (consisting of mainly Nb and Al) that was used to make the VAR electrode. The presence of the large TiC based inclusion within the disc is rather more difficult to explain. The various methods used to bring carbon additions into ingots are kept secret and thus very little information is openly available. However, one method of incorporating carbon into ingots, via the use of master-alloys, and employing fine TiC powder is described in [13]. Although it is not known how carbon was incorporated into the ingots used in the present study, it could be speculated that a similar method was used and that the large TiC-based inclusion found in the forged disc resulted from the TiC containing master alloy that was used to dope the alloy with carbon. As the melting point of TiC is around 3170°C, dissolution of such a large TiC-based particle would be almost impossible.

3.4 Mechanical properties of three-step hot-worked material

The results of the room temperature tensile tests and schematic diagrams illustrating how the specimens were orientated within the large disc are shown in Fig. 14. The black curves are for material that was tested in the as-forged + annealed (1030°C/4 h/furnace cool) condition. The grey tensile curves are for material that was given an additional heat treatment of 1280°C/30 min/air cool + 800°C/6 h/furnace cool. This heat-treatment was performed in order to establish a precipitation hardened near-lamellar microstructure in the material. The heat-treatments were performed on cylindrical test-piece blanks and the specimens subsequently made from the heat treated cylinders.

Figures 14a and 14b show that the as-annealed material generally exhibited appreciable ductility, showing between 1.2 and 1.7 % plastic elongation when the specimens were orientated within the plane of the disc. These values compare well to the value of 1.3 % that was measured by Draper et al. [10] parallel to the extrusion direction of a double extruded bar of the same alloy. However the strength levels, $\sigma_{0.2\%}$ and σ_{UTS}, measured for the double extruded material are around 225 MPa and 245 MPa higher than the values reached in Figs. 14a and 14b. Although the alloy studied by Draper et al. [10] and that in the present study have the same nominal composition, differences cannot be

excluded, especially considering the compositional profile shown in Fig. 5. The higher aluminium content indicated in Fig. 5 would lead to a lower strength, as discussed by Paul et al. [1]. In addition, the microstructure of the double extruded material and the annealed as-forged material are quite different. The double extruded material had a duplex microstructure containing a high fraction of lamellar colonies with a grain size of approximately 20 μm and a small volume fraction of fine, ≈ 4 μm, gamma grains located between the lamellar colonies and at the periphery of the extruded bar. This is somewhat unlike the microstructure of the as-forged + annealed material, shown in Fig. 7, which contained isolated grains of α_2 in a γ matrix. Such differences in microstructure could be explained by either a lower aluminium level in the double extruded bar and/or the higher temperature (1280°C) used for extrusion compared to that used during the isothermal forging (1150°C). Rather disappointingly one tensile test in Fig. 14a exhibited brittle fracture at a stress of 480 MPa. Figure 13 shows the fracture face of this specimen, observed using both SE (secondary electron) and BSE (back scattered electron) scanning electron microscope imaging modes, where it can be seen that a large defect was responsible for the premature fracture.

Due to their shorter length, the through-thickness tests specimens were tested without an extensometer using displacement control, at an initial strain rate of 2.38×10^{-5} s^{-1}. This is the reason why the apparent Young's modulus is only around 50 % of that measured for the specimens tested using strain control. In the through thickness direction, the annealed material exhibited brittle behaviour with fracture stresses of 650 MPa or higher, Fig. 14c.

On comparing the tensile properties of the near alpha-transus heat-treated material to those of the annealed material, it can be seen that the yield stress is around 100 MPa lower after the near alpha-transus heat-treatment, Figs. 14a and 14b. Nevertheless, the fracture stresses of the different microstructures were similar, although the ductility levels were slightly lower compared to the annealed material, varying from 0.9 to 1.1 %. A positive effect of the near alpha-transus heat-treatment is that some plastic elongation, 0.6 to 0.7 %, was measured for specimens tested in the through-thickness direction, Fig. 14c. In contrast no ductility was measured for the through-thickness specimens in the as-forged and annealed condition. This type of behaviour is very similar to the differences observed in extruded bar with fine (as-extruded) and nearly fully-lamellar (transformed) microstructures, when tested parallel and transverse to the extrusion direction [14]. Very interestingly, after the near alpha-transus heat-treatment, the yield strength was independent of sample orientation, Figs. 14a to 14c, indicating isotropic behaviour.

In the work of Draper et al. [10], a fully lamellar microstructure in the double extruded material was obtained via a heat-treatment 30°C above the alpha-transus temperature, while in the current study heat-treatment at a temperature slightly below the alpha-transus temperature was employed. This, combined with the effect of any compositional differences, is reflected in the much larger mean colony size (325±45 μm colony diameter) of the double extruded material after transformation compared to that obtained in the present study (see the microstructure on either side of the band defect in Fig. 10). Such microstructural differences may explain the roughly 70 MPa higher value for σ_{UTS} (Figs. 14a and 14b) that was obtained in the current study as compared to that determined by Draper et al. [10]. Additionally, the associated plastic elongations in the present study (around 1 %) are significantly higher than the mean value of only 0.31 % determined by Draper et al. [10] on material heat-treated above the alpha-transus temperature.

3.5 Quality issues associated with ingot production

Both the current study and that of Porter et al. [15] indicate that in spite of extensive hot working, large differences in macro-composition can, at best, only be reduced and not eliminated. If a near alpha-transus heat-treatment had been performed in the current work on the forging billets that were cut from the extruded bar, then the degree of segregation within each forged stacking element disc would certainly have been reduced. Such a heat-treatment has been shown to improve the ductility of subsequently forged material [16]. However, such a treatment would not reduce any compositional differences between different billets taken from different parts of the extruded bar. Due to the very large diffusion distances necessary to remove macro-segregation within large ingots, both end to end, and centre to surface; it is almost impossible to remove such compositional differences even through the use of long term near- or above alpha-transus heat-treatments. Thus the extent of elemental homogeneity within ingots is a crucial factor regarding quality of final products. In the present study both the variation of microstructure, Figs. 1 and 2, and composition across the extruded bar, Fig. 3, indicate that macro-segregation in the ingots used was much higher than desirable. Thus the ability of ingot manufacturers to produce defect-free ingots, particularly large ones, with significantly reduced macro-inhomogeneity remains a key technological area where much work is still required. The ability to consistently obtain the correct mean ingot composition is also extremely important. Figure 5 indicates that the mean composition of one of the small forged plates contained over 1 at.% more Al than the nominal composition. This could arise from either the mean Al content of the ingot being too high (resulting from the loss of Al during the VAR processing being less than anticipated) or from significant macro-segregation. On account of the fact that all the elemental scans indicated an excess of Al, the first explanation seems more likely although a contribution from macro-segregation cannot be completely excluded.

In the literature two main techniques have been used to melt large titanium aluminide ingots, namely plasma arc melting (PAM) [15] and vacuum arc melting (VAR) [13]. Another method that has often been employed to make small to medium size ingots, and that has also been used for melting prior to investment casting is induction skull melting (ISM) [17]. With regard to macrosegregation in a single melted 8 cm diameter PAM ingot, Godfrey and Loretto [12] identified that the macrosegregation pattern did not correspond to that expected from solidification but resulted from the heterogeneous nature of the feedstock which comprised of pucks made from compacted raw materials. In order to reduce macrosegregation, it was recommended that the pucks be made from fine-sized material and that multiple meltings be performed. To further improve ingot macro-homogeneity it was recommended that the size of the melt hearth be as large as possible, and/or that multiple hearths be used in order to ensure that a homogeneous melt flows into the crucible. For the vacuum arc melting (VAR) technique it is reported that master-alloys are used to aid the dissolution of high melting point elements into the ingot via lower melting point materials [13]. According to this work, so-called 2xVAR processing of a 15 cm long by 7 cm diameter ingot, resulted in Al deviations of about ± 0.5 at.%. The ISM technique involves the simultaneous melting and mixing of elemental and/or master-alloys within a water-cooled induction crucible [17]. It is reported that the induction field leads to intense stirring of the melt which promotes melt homogeneity prior to casting. Starting from un-alloyed charge material, the variation of Al from top to bottom of a 7 cm diameter by 86 cm long bar-shaped ingot is reported to be 0.29 wt.%, which for Ti-48Al-2Cr-2Nb is equivalent to around 0.35 at.%. This variation in Al, and that reported above for the 2xVAR ingot, are rather low; however it should be remembered that considerably larger variations are likely in ingots of increasing size. Using current manufacturing philosophies such large ingots are required to make large parts.

In unpublished work performed at HZG (formerly GKSS), values of Al were seen to vary by 0.3 at.% from the centre to the outer surface of a 14 cm diameter PAM ingot. A corresponding value of 1 at.% was measured for a somewhat larger 22 cm diameter VAR ingot. Although the end to end variation was not determined for the VAR ingot, a variation of up to 2 at.% was determined for the PAM ingot. Variation of composition, particularly of Al, is an important factor that leads to microstructural and property variations, and as such must be minimised. Porter et al. [15] used x-ray imaging to show that elemental segregation remained in a forged disc even after prior extrusion and a high temperature heat-treatment of 1370°C for 5 hours. The initial PAM ingot used in the work had a diameter of 35.6 cm which was required in order to obtain an extruded bar with a diameter

sufficiently large enough to produce a forged disc of the required size [15]. This work exemplifies the problems in the manufacture of large components.

Until a time when the quality of large ingots can be assured, the multi-stage hot working technique that has been presented here may be employed to obtain high quality components. Success critically relies on being able to use non destructive examination techniques (NDE) to identify semi-finished products (i.e. the small forged discs) that are unsuitable for further processing on account of defects. However this is not an easy task because the critical defect size is small and the defects are relatively rare, a little like searching for a needle in a haystack. The NDE techniques must be capable of reliably detecting structural and chemical inhomogenities that may only be a few microns in size. The question nevertheless exists how to achieve this. Here it is worth noting that the ground forged plates with parallel end faces are particularly suitable for some examination techniques. Indeed the use of much smaller cast ingots that are currently available could have certain advantages compared to using large ingots, including reduced macro-segregation and a finer as-cast microstructure. Even if the extrusion processing step was not employed on account of the very small diameter of the resulting extrudate, the use of multi-step forging could nevertheless achieve imparted strain deformations of up to around 3 which are still very high, and probably sufficient to fully recrystallise the initially finer as-cast microstructure and result in acceptable properties.

4 Conclusions

In order to use large TiAl components such as discs, the absence of defects and significant elemental macro-segregation, as well as properties must be guaranteed. State of the art manufacture of the large ingots required is not able to meet these challenges and further work is required to improve the situation. A number of defects have been found in the present investigation and their origin discussed. A new method that, when combined with suitable and effective NDE techniques, has the capability to produce high quality products such as discs or BLISKS is presented. In this regard any interested parties are welcome to contact the authors to make a demonstration component from the remaining large disc.

References

1. Paul JDH, Appel F and Wagner R. Acta Mater 1998; 46: 1075.
2. Mishin Y and Herzig C. Acta Mater 2000, 48: 589.
3. Witusiewicz VT, Bondar AA, Hecht U, and Velikanova T-Ya. J Alloys Comp 2009; 472: 133.

4. Oehring M, Paul JDH and Appel F. US Patent 2011; US 7,870,670 B2.

5. Semiatin SL, Segal VM, Goetz RL, Goforth RE, and Hartwig T. Scr Metall Mater 1995; 33: 535.

6. Sastry SML, Mahapatra RN and Hasson DF. Scr Mater 2000; 42: 731.

7. Sastry SML and Mahapatra RN. Mater Sci and Eng A 2001; A329-331: 872.

8. Appel F, Buque C, Eggert S, Lorenz U, Oehring M, and Paul JDH. In: Kim Y-W, Clemens H and Rosenberger AH, editors. Gamma Titanium Aluminides 2003. TMS Symposium Proceedings, Warrendale, PA, 2003, p. 319.

9. Fröbel U and Appel F. Metall Mater Trans A 2007; 38A: 1817.

10. Draper SL, Das G, Locci I, Whittenberger JD, Lerch BA, and Kestler H. In: Kim Y-W, Clemens H and Rosenberger AH, editors. Gamma Titanium Aluminides 2003. TMS Symposium Proceedings, Warrendale, PA, 2003, p. 207.

11. Herrmann and Appel F. Metall Mater Trans A 2009; 40A: 1881.

12. Godfrey B and Loretto MH. Mater Sci and Eng A 1999; A266: 115.

13. Güther V, Otto A, Kestler H, and Clemens H. In: Kim Y-W, Dimiduk DM, and Loretto MH, editors. Gamma Titanium Aluminides 1999. TMS Symposium Proceedings, Warrendale, PA, 1999, p. 225.

14. Appel F, Paul JDH and Oehring M. Gamma Titanium Aluminides, Science and Technology, Weinheim, Germany: Wiley-VCH, 2011, p. 636.

15. Porter WJ, Li K and Rosenberger AH. In: Kim Y-W, Dimiduk DM and Loretto MH, editors. Gamma Titanium Aluminides 1999. TMS Symposium Proceedings, Warrendale, PA, 1999, p. 587.

16. Koeppe C, Bartels A, Seeger J, and Mecking H. Metall Trans A 1999; 24A: 1795.

17. Reed S. In: Kim Y-W, Wagner R and Yamaguchi M, editors. Gamma Titanium Aluminides. TMS Symposium Proceedings, Warrendale, PA, 1995, p. 475.

Figures

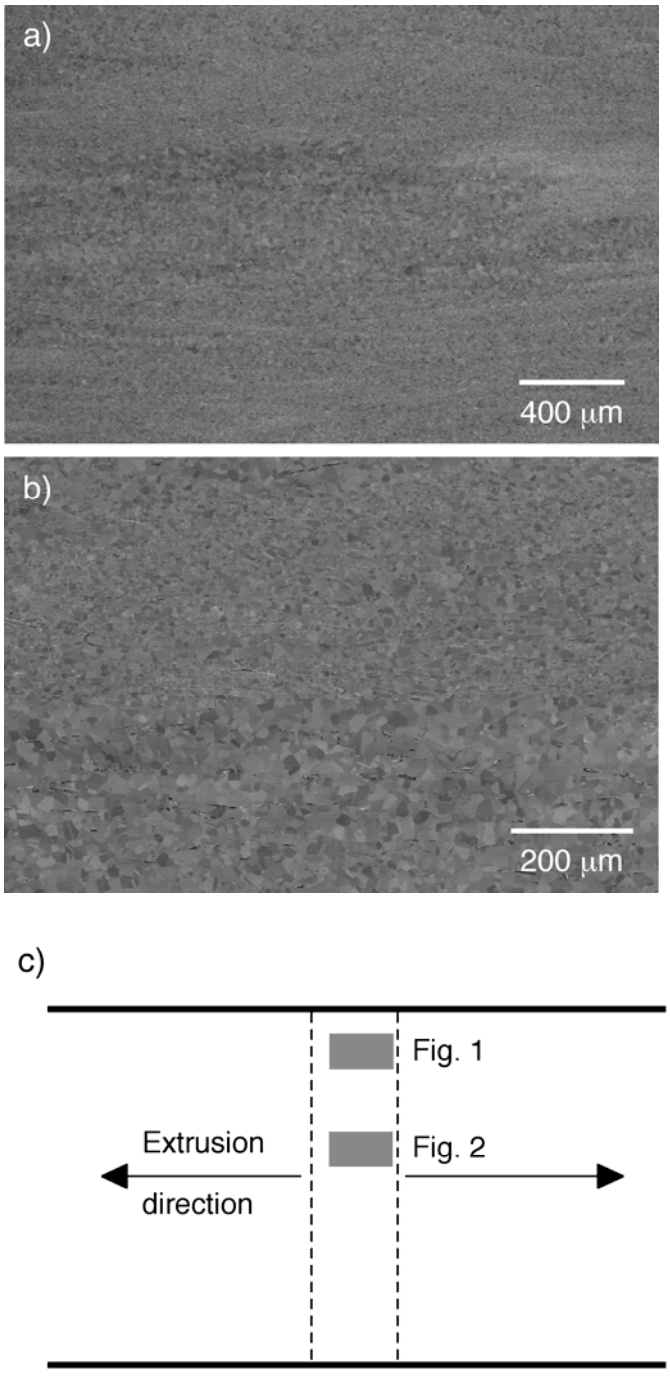

Figure 1: Microstructure of the annealed extruded bar (extrusion direction is horizontal): (a) Close to the outer surface of the bar showing both fine and coarse-grained banded regions. (b) Illustrates a boundary region between fine- and coarse-grained bands in higher magnification. The composition of the fine-grained area in (b) was Ti-46.9Al-4.9Nb and that of the coarse-grained area was Ti-47.6Al-4.7Nb. Such compositional differences result from the solidification process and can be particularly significant and large in size for big ingots. Although difficult to see, there were many more borides present in the Al rich microstructure. Figure 1c indicates the rough positions within the extruded bar where the microstructures shown in Figs. 1 and 2 were observed.

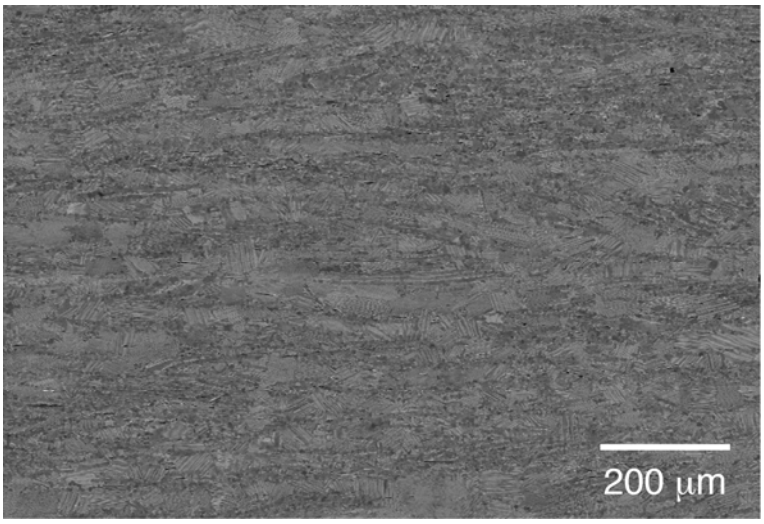

Figure 2: Microstructure close to the centre of the annealed extruded bar showing a predominantly fully lamellar microstructure but with a certain degree of fine-grained microstructure between the lamellar regions. Figure 1c shows the approximate position within the extruded bar at which the micrograph was taken. The degree of microstructural inhomogeneity within the extruded bar can be seen by comparing Figs. 1 and 2. The extrusion direction is horizontal.

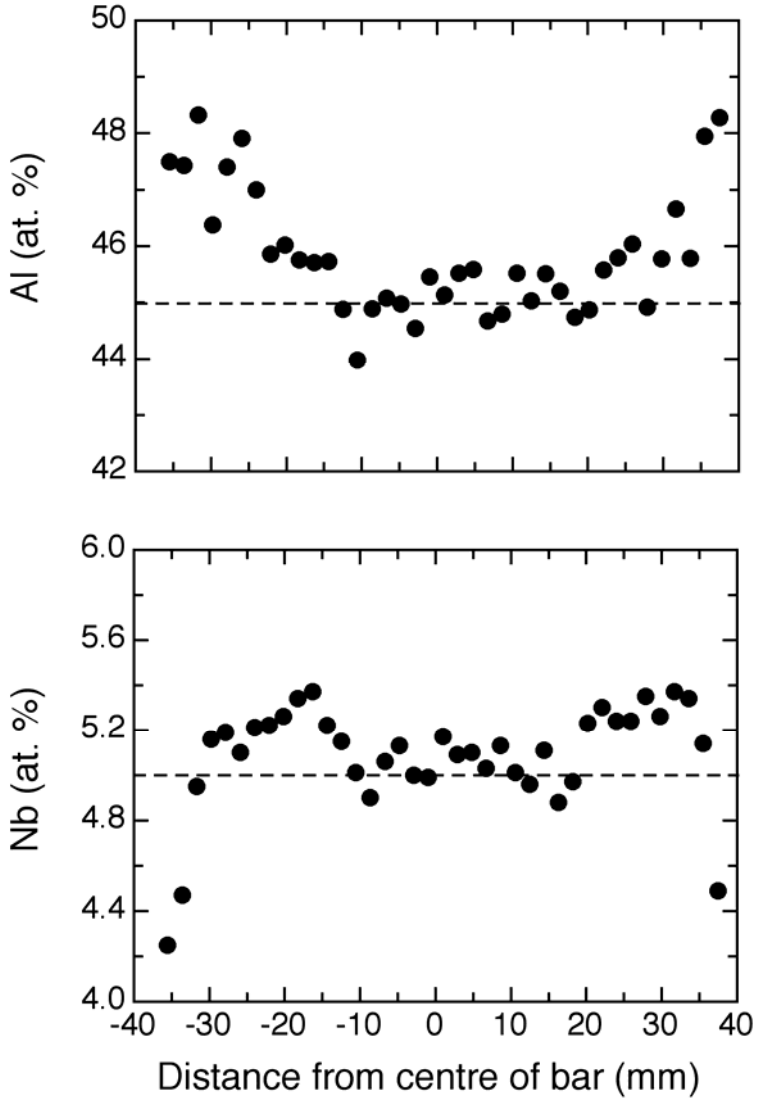

Figure 3: Graphs showing the distribution of Al and Nb through the cross-section of the annealed extruded bar. Each point represents the mean elemental concentration determined from an area of 1.08 mm^2. A marked variation of Al across the bar can be seen. The significantly lower Al content near the centre of the bar would explain the marked variation in microstructure seen between Figs. 1 and 2. The dashed lines indicate nominal composition values.

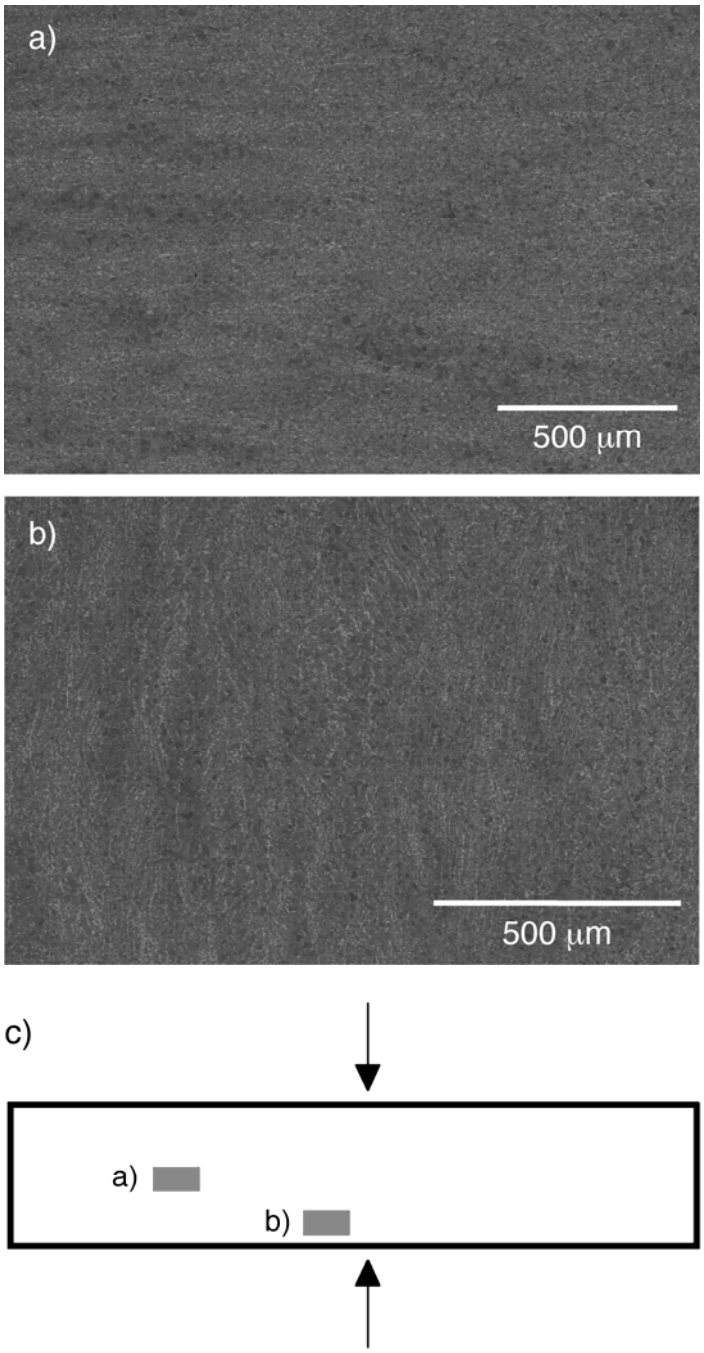

Figure 4: Microstructure within an annealed small forged disc that was made from a billet that had been cut from the annealed extruded bar. The forging direction (and also the extrusion direction) is vertical in all figures. Figure 4a was taken from an area close to the rim of the disc and shows banding that is preferentially orientated perpendicular to the forging direction. Figure 4b was taken from an area near to the centre of the disc and close to the contact area with the forging die. In this region microstructural banding is orientated parallel to forging direction and is probably related to the aligned extruded microstructure. Figure 4c indicates the approximate positions within the small forged disc where the micrographs in Figs. 4a and 4b were taken.

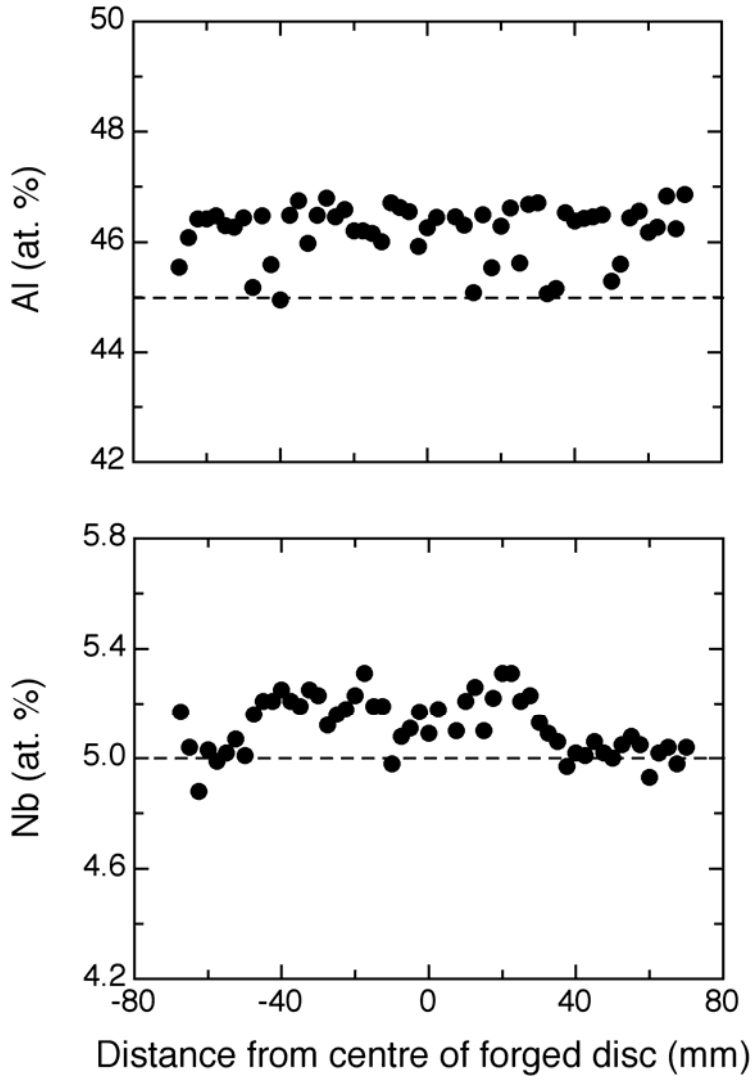

Figure 5: Graphs showing the distribution of Al and Nb from rim to rim and through the centre of an annealed small forged disc. The overall Al homogeneity is better than that of the extruded bar, but nevertheless areas that differ in Al by up to 2 at.% remain. The dashed lines indicate nominal composition values.

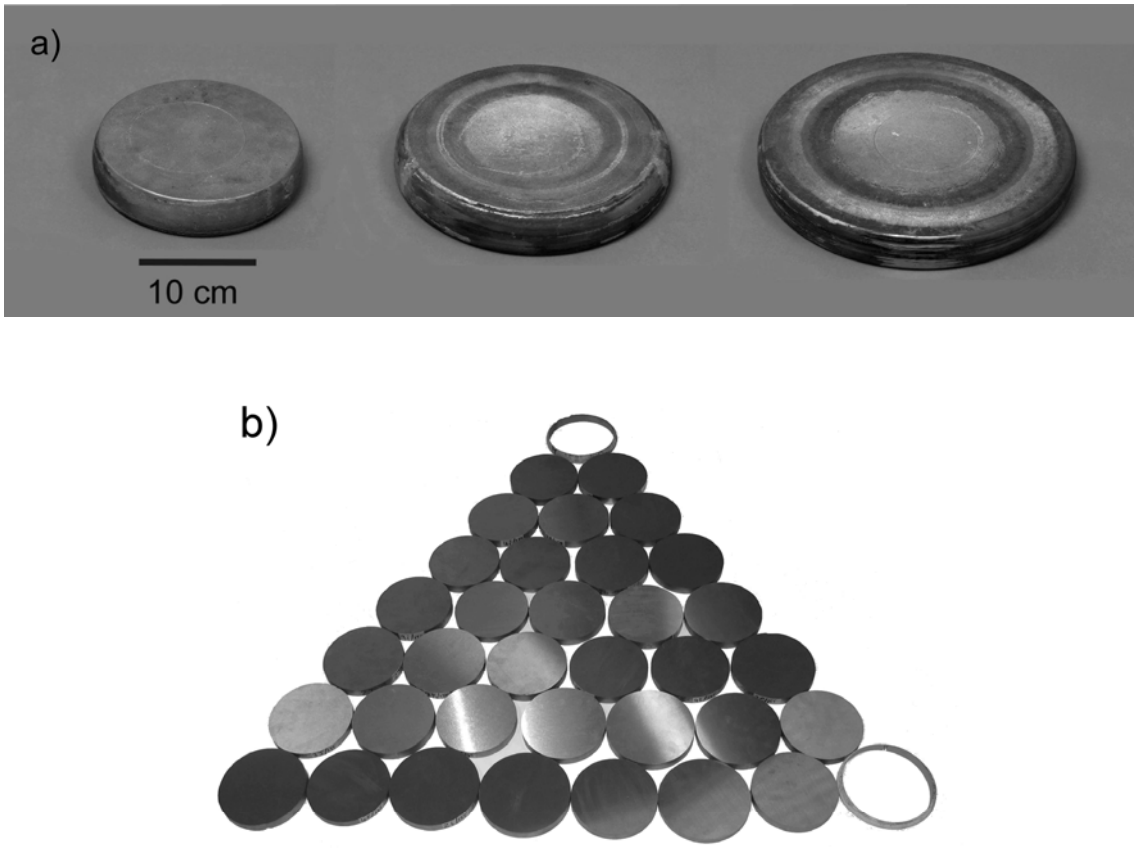

Figure 6: a) Photograph of the 3 large TiAl discs that were made in the project. The metallographic and mechanical test specimens were taken from the middle disc which had an unsymmetrical shaped rim. b) Shows a number of the small forged discs that were used to make the stacked assemblies that were encapsulated prior to HIP bonding. These small discs had diameters of 14.5, 15.0 or 15.5 cm and were between 14 and 19 mm in thickness. The rings at the top and right-hand corners of the triangle shape are what remain after the discs were cut from the forged plates.

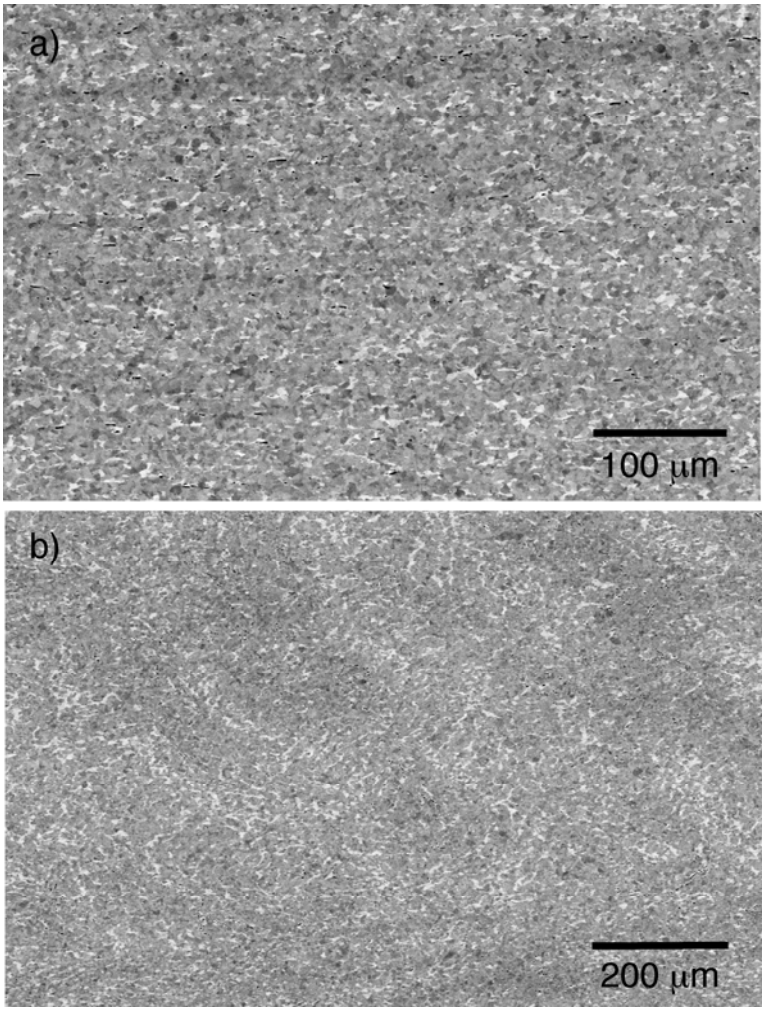

Figure 7: Microstructure of the second largest disc, as-forged condition; the forging direction is vertical in both micrographs. (a) Shows that the microstructure is preferentially aligned perpendicular to the forging direction, whereas (b) shows a “mottled” microstructure with a less well defined orientation with respect to the forging direction.

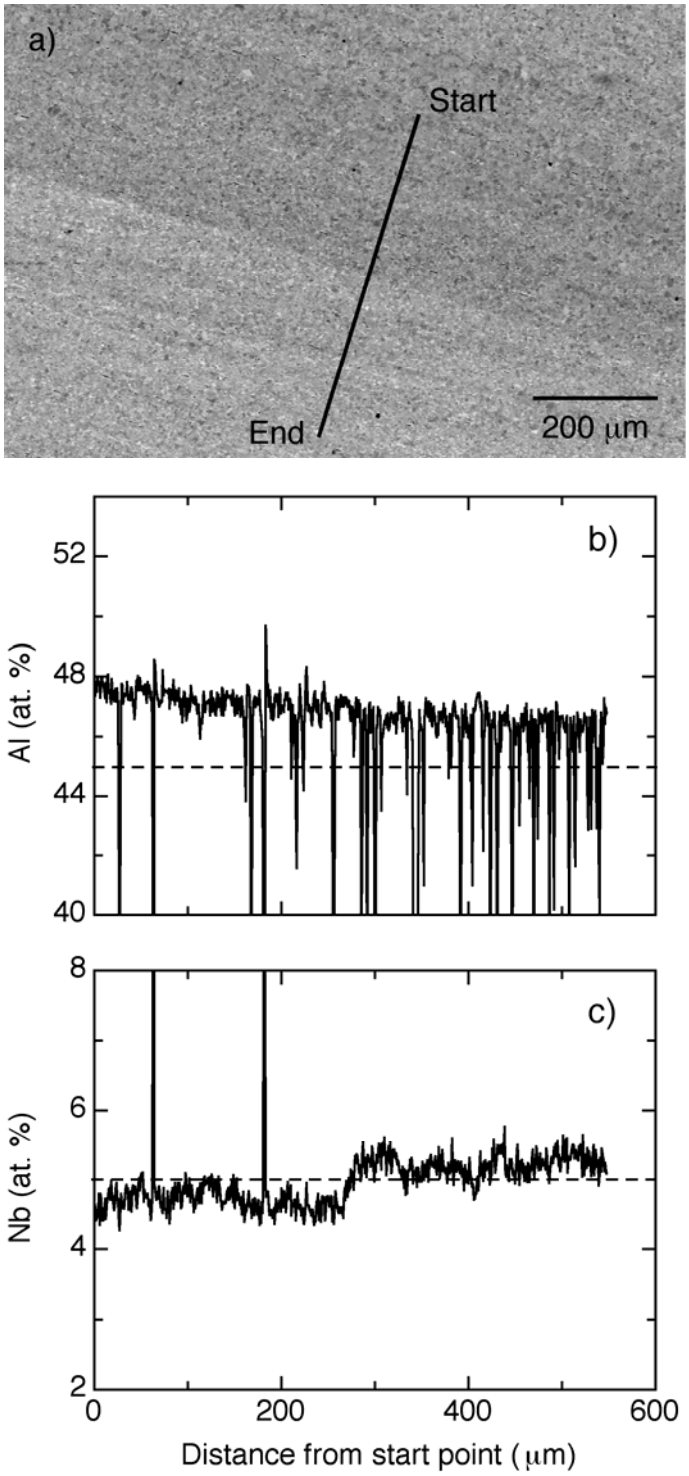

Figure 8: (a) Micrograph from the large as-forged disc showing the position of an interface between two former (small forged-disc) stacking elements. The interface can be deduced from the position where the volume fraction of light-coloured α_2 phase suddenly changes. The position of an elemental (point) line scan analysis is indicated in the micrograph and the results for Al and Nb given in (b) and (c) respectively. The position of the interface is clearly indicated by a sudden change in the Nb level. The dashed lines indicate nominal composition values.

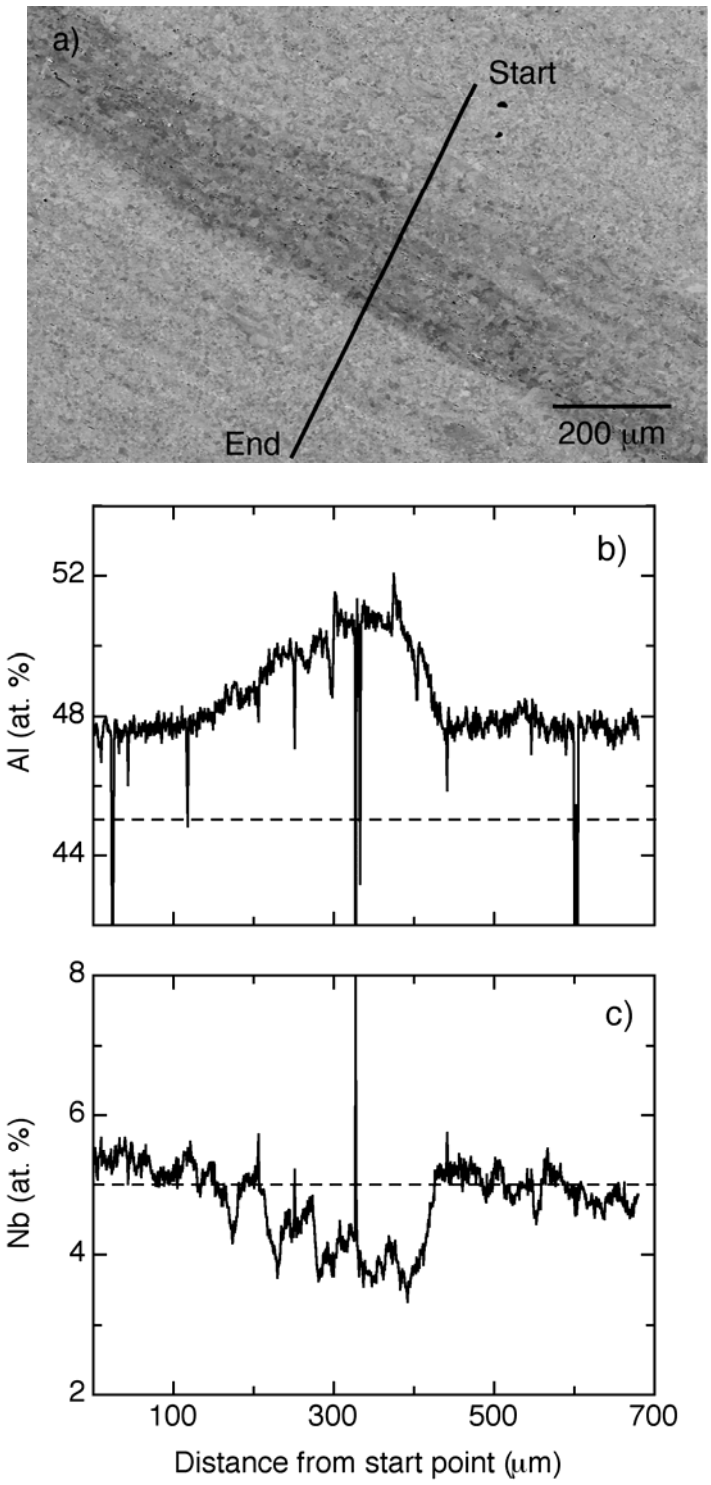

Figure 9: (a) Micrograph showing one of the most extreme cases of elemental segregation that was found within the large as-forged disc. The position of an elemental (point) line scan analysis that was performed is indicated in the micrograph and the results for Al and Nb are given in (b) and (c) respectively. The dashed lines indicate nominal composition values.

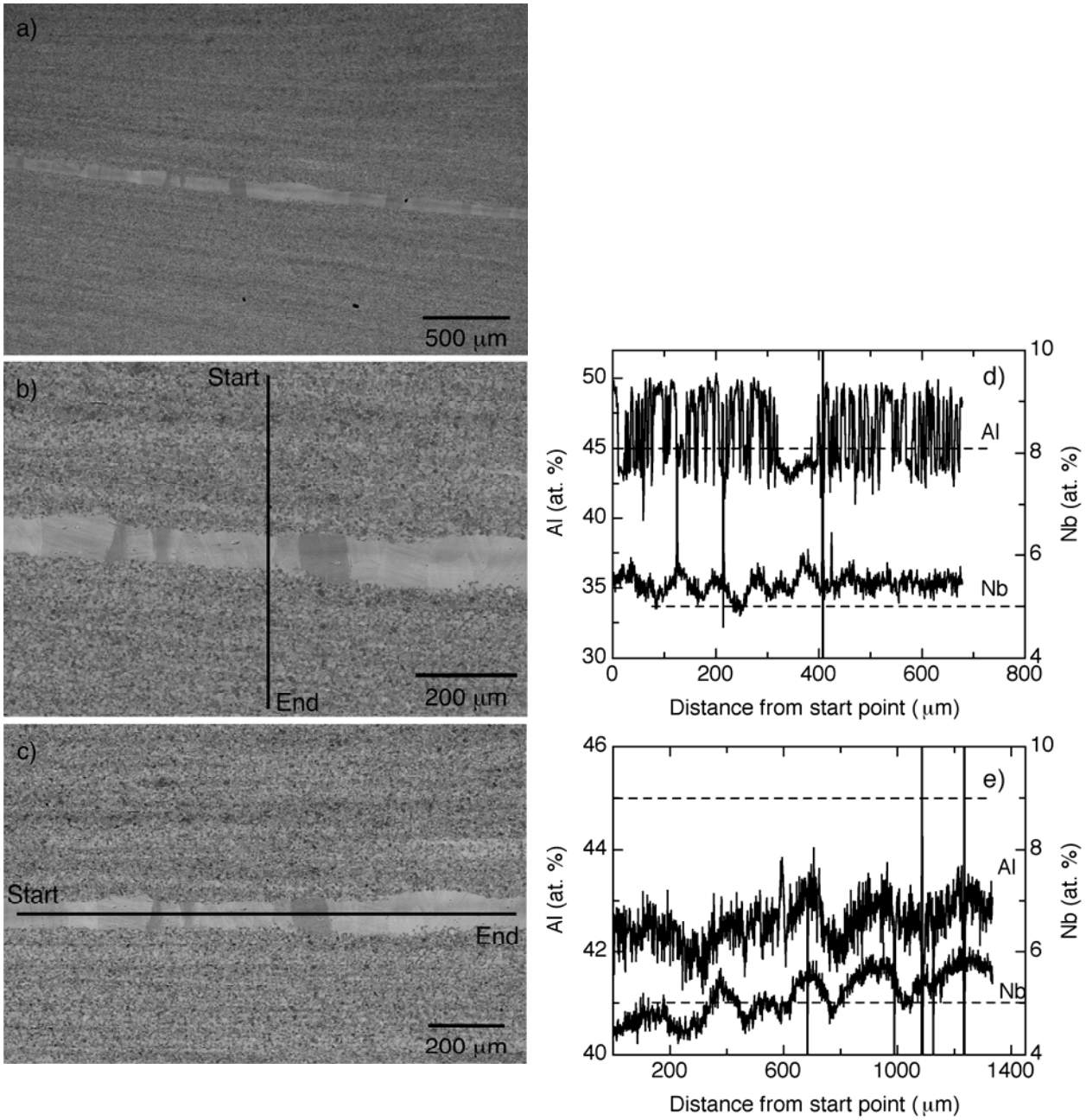

Figure 10: (a) Micrograph showing an Al-poor band that extended several mm in length within the large forged disc (specimen given a near alpha transus heat-treatment). (b) and (c) indicate the positions where elemental (point) line scans were performed. The results for the scan passing from the matrix and then through the band (b) are shown in (d), while those for the scan taken along the band (c) are shown in (e). The dashed lines indicate nominal composition values.

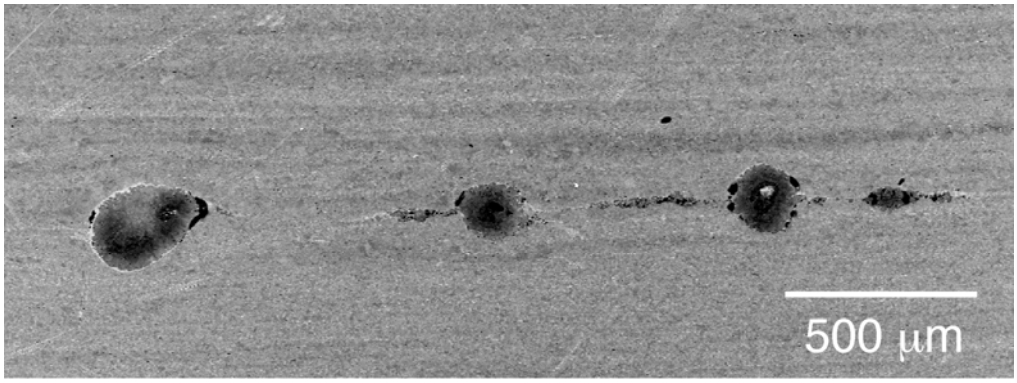

Figure 11: Large Ti-rich/Al-poor inclusions in the large as-forged disc.

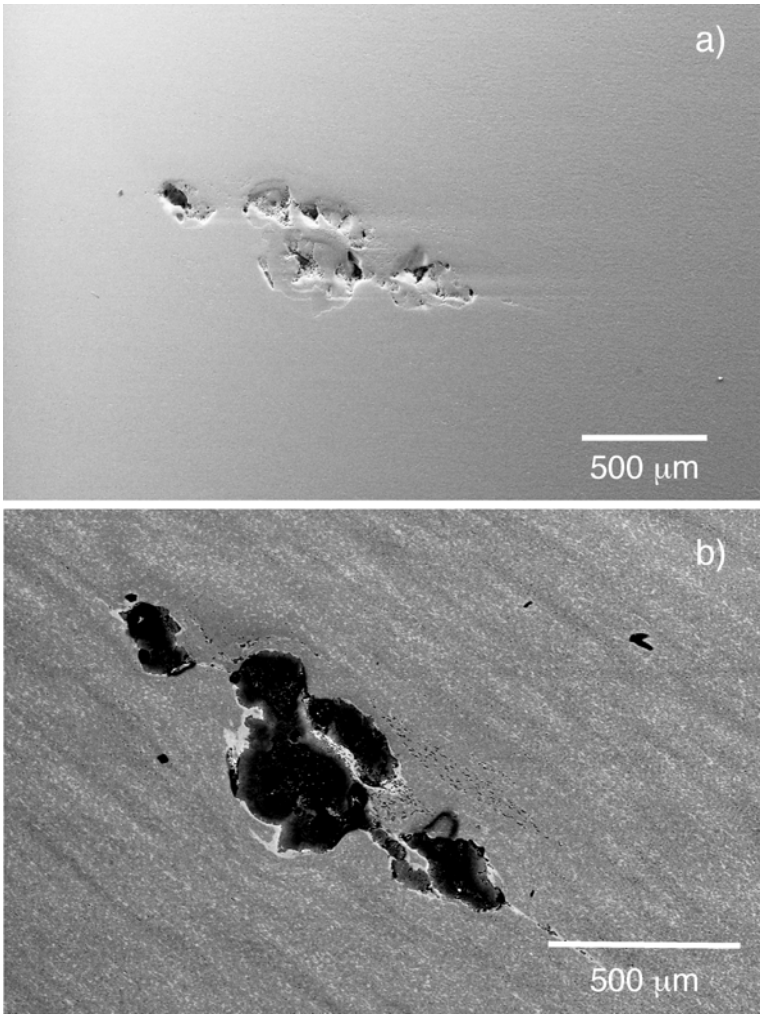

Figure 12: (a) A large “apparent crack” that is actually an inclusion on the polished surface of a metallographic specimen that was taken from the large as-forged disc. The defect, which was also visible to the eye, is imaged using the SE mode. (b) The same defect imaged in BSE mode. EDX mapping showed the presence of both Ti and C indicating that the inclusion was probably TiC based.

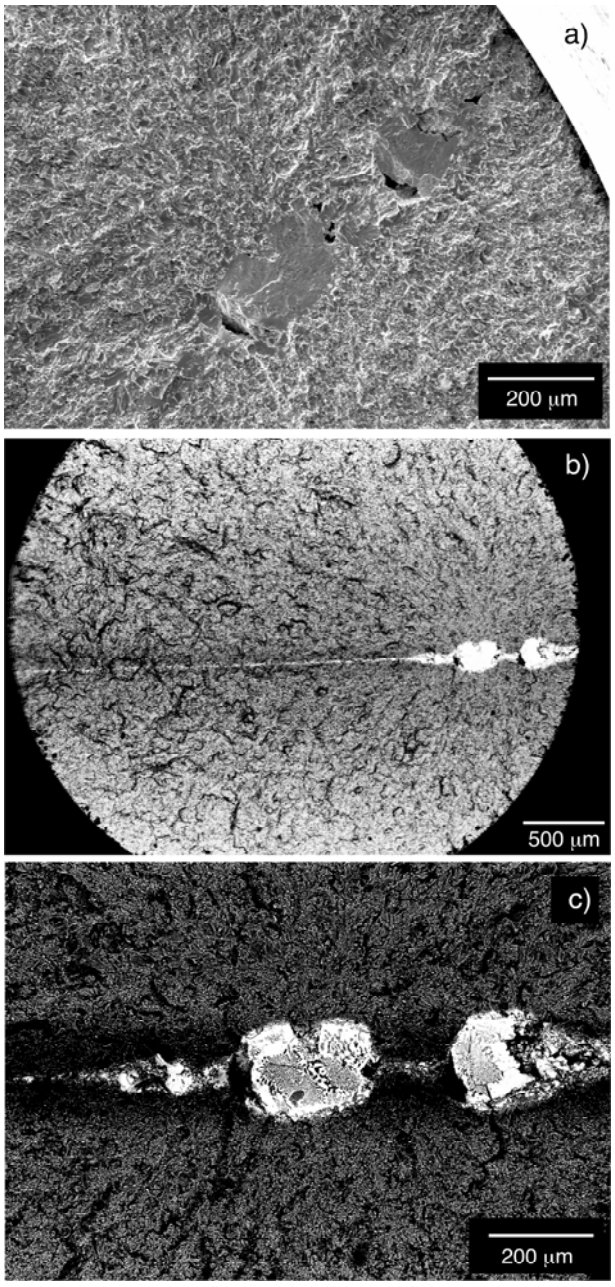

Figure 13: (a) Fracture surface of the tensile test specimen that broke at 480 MPa, see Fig. 14a, imaged using SE mode. (b) The same fracture surface imaged using BSE mode. It can be seen that very large inclusions are present on the fracture surface and are very likely the reason for the premature failure. The large amount of deformation that has been imparted into the disc can be seen from the length of the inclusion tails which extend over the whole 3.5 mm specimen diameter. Although EDX cannot be performed on a fracture face, the light colour of the defect indicates it is rich in heavy elements such as Nb or Ti. (c) Higher magnification of the inclusions, showing them to have a two phase nature.

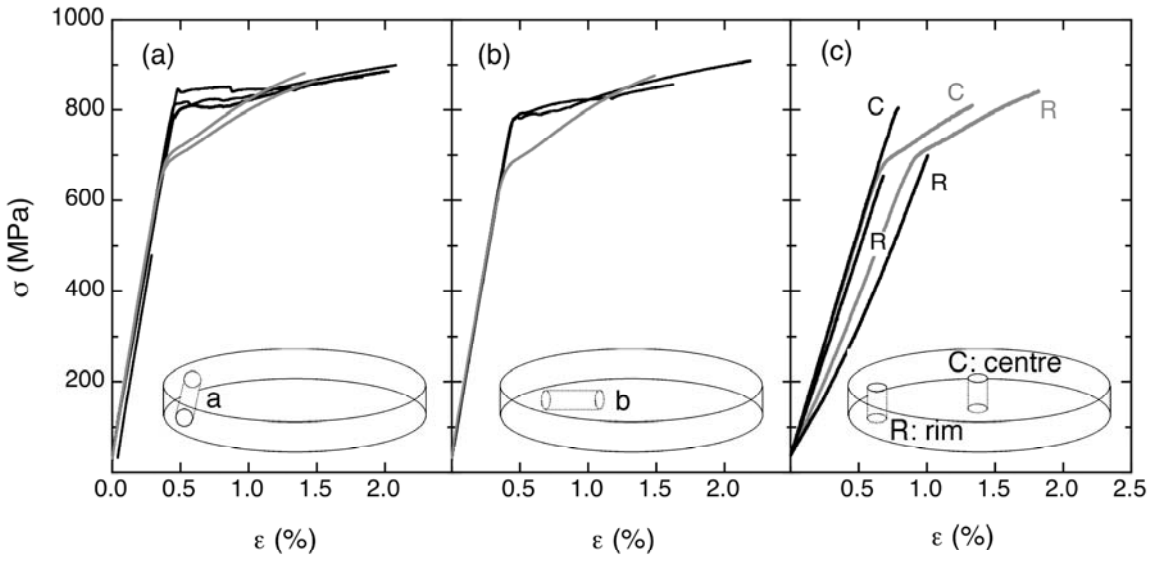

Figure 14: Room temperature tensile test curves for specimens that were taken from the large forged disc. The orientation of the specimens is indicated in the diagrams. The black lines are for the as-forged + annealed (1030°C/4 h/furnace cool) condition, whereas the grey lines are for material that was annealed and subsequently heat-treated close to the alpha-transus temperature (1280°C/30 min/air cool) and then precipitation hardened (800°C/6 h/furnace cool). The curves for through-thickness specimens (Fig. 14c) are labelled with R to indicate that the specimens were taken from near to the disc rim, while C indicates that the specimens came from near the centre of the disc.